Available online at www.sciencedirect.com
SCIENCE DIRECT®
Journal of Nuclear Materials 341 (2005) 209–223
journal of nuclear materials
www.elsevier.com/locate/jnucmat

Uranium secondary phase formation during anoxic hydrothermal leaching processes of UO_2 nuclear fuel

M. Amme [a,*], T. Wiss [a], H. Thiele [a], P. Boulet [a], H. Lang [b]

[a] European Commission, Joint Research Centre, Institute for Transuranium Elements, Postfach 2340, D-76125 Karlsruhe, Germany
[b] GSF National Research Centre for Environment and Health, formerly Institute of Hydrology, Ingolstädter Landstr. 1, D-85764 Neuherberg, Germany

Received 9 June 2004; accepted 28 February 2005

Abstract

Mobilisation of uranium in geologic environments from UO_2 solid phases usually takes place by oxidative dissolution involving a change of U oxidation state from +IV to +VI; however, anoxic or reducing geochemical conditions are expected in many of the planned European disposal sites. This work investigates potential alteration mechanisms of UO_2 in contact with groundwater ions (Ca^{2+}, CO_3^{2-}, and silicate) under anoxic conditions, at ambient (25 °C) and hydrothermal (180 °C) temperature conditions. SEM–EDX analysis detected (in the case of treatment at 180 °C in high silicate content solutions) a compound with U:Si ratio of 1:1 on the UO_2 surfaces after leaching. Minor quantities of phases containing U, Ti, Fe, Si, and Ca were formed, these could not be characterized completely. A further experiment, performed in the presence of dissolving $CaO/TiO_2/SiO_2/Fe(0)–Fe_2O_3$, formed a compound with U:Si:Ca of 1:2:8, a ratio not matching any known uranyl compound. The two phases, possibly identical with coffinite, $USiO_4$, and U-bearing ekanite, $UCa_2Si_8O_{20}$, were found to form at different [Ca]/[Si] conditions. The implications upon the final geologic storage of actual, heterogeneous spent fuel are discussed.

1. Introduction

The final disposal of spent nuclear fuel in deep geologic formations is considered as waste management option in several European states. Conservative assessment procedures foresee that the containments that store the fuel may fail and the radioactive material might come into contact with intruding groundwater. The boundary condition for radionuclide release (the so-called 'source term') operates with several parameters on the base of which the dissolution process is estimated. One important parameter is the chemical nature of the solid–liquid interface between spent nuclear fuel and groundwater. The composition of the outer solid layer is regarded as the solubility-controlling factor; therefore there is considerable interest in the physical and chemical properties of secondary phases which could be formed during the contact with water.

European sites under investigation for final disposal are for the greatest part located in such depths that the surrounding environment, if undisturbed, is considered as oxygen-free (anoxic) [1,2]. The factor of oxygen partial pressure plays an important role for the development of uranium chemistry during material alteration. Spent

* Corresponding author. Tel.: +49 7247 951148; fax: +49 7247 951593.
E-mail address: amme@itu.fzk.de (M. Amme).

0022-3115/$ - see front matter © 2005 Elsevier B.V. All rights reserved.
doi:10.1016/j.jnucmat.2005.02.004

nuclear fuel consists predominantly of a UO_2 matrix that contains a variety of fission products and actinides in minor concentrations; therefore, uranium solid phases (particularly products of an alteration sequence starting with UO_2) are to be expected. Newly formed phases generated by a corrosion process on UO_2 were observed for oxic environments in many cases [3,4]. Then, the quadrivalent uranium in UO_2 is converted almost completely into the hexavalent state, UO_2^{2+}. However, for disposal conditions discussed here, the geochemical boundary parameters would favour the formation of quadrivalent uraninite alteration phases due to the absence of oxygen and low redox potentials [5,6]. The formation of such solids in aqueous solution proceeds more slowly than the oxidative formation of U(VI). It is therefore rarely observed in laboratory timescale experiments but commonly found in natural analogue materials [7,8]. As a consequence, the number of investigations that deal with uranium(IV) secondary phase formation from anoxic UO_2 dissolution experiments is very limited.

Uranium(IV) phases (others than uraninite) appear frequently in geologic media and, additionally, U(IV) is found as a component of minor concentration in many mineral phases. The phases that can form during hydrothermal processes are of special interest for the final repository investigations, because temperatures close to the fuel surface may well rise above 100 °C during the first thousands of years, depending on the geometry of material, containment arrangement and near field isolation. At later times (>10^4 years), intrusion of hot fluids and geothermal gradients can have an impact on the composition of the stored material. As an example, the phases coffinite ($USiO_4 \cdot nH_2O$), brannerite ((U,Ca,Ce,Y)[(Ti,Fe)$_2O_6$]), and ekanite ((Th,U)(Ca,Fe)$_2Si_8O_{20}$) can form at hydrothermal conditions in geologic media [9]. For the case of coffinite formation, further mechanisms were found to apply [10]. These materials can be seen as potential candidates for uranium(IV) secondary phases formation during anoxic spent fuel alteration. Special attention is given to them in the present work.

For the investigation, three mechanisms of anoxic UO_2 alteration were selected that were observed formerly with geologic analogue materials, and may take place also in deep repository environments (shown in Fig. 1) [11–13]: enhanced dissolution by and possible secondary phase formation with carbonate ions, incorporation of calcium cations into the UO_2 lattice, and the formation of uranium(IV) silicate ($USiO_4$, coffinitization). Three types of experiments were performed: Nuclear-grade unirradiated UO_2 material (used as analogue for spent nuclear fuel) was exposed at 25 °C and anoxic conditions (Ar atmosphere) to solutions of a natural groundwater spiked with enhanced concentrations of Ca^{2+}, CO_3^{2-}, and SiO_2 (aq). Secondly, experiments were repeated at 180 °C in sealed autoclave vessels. The first experiment was intended to investigate water chemistry

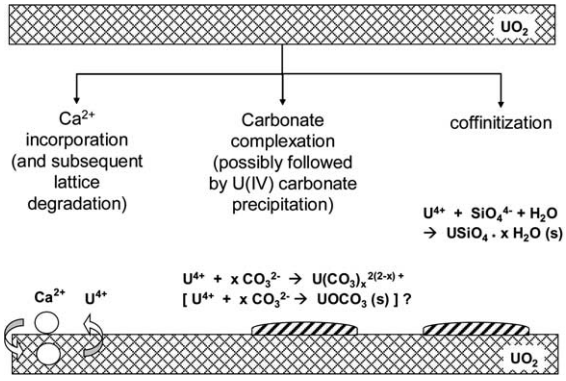

Fig. 1. Potential alteration pathways of UO_2 in contact with groundwater in anoxic environments.

effects (influence of different ions) on the UO_2 dissolution in order to determine a possible effect that might lead to anoxic secondary phase formation. Geochemical parameters and U oxidation states were measured before and after the experiment. The second set used hydrothermal conditions in order to take advantage of higher reaction rates of solids formation at elevated temperatures. A third test was intended to investigate the reaction pathways of preferential secondary phase formation. Therefore, samples of powdered and pellet-form UO_2 were heated in groundwater solution to 180 °C in the presence of solid SiO_2, Fe(0)/Fe_2O_3, TiO_2, and CaO, in such way providing an unlimited amount of Fe^{2+}, Ca^{2+}, Ti^{4+}, and SiO_2 (aq) continuously supplied into solution. All solutions were characterized for uranium concentration after the experiments. Additionally, the distribution of uranium oxidation states in solution, as well as the geochemical parameters pH and Eh were determined for the first set of experiments. All solid samples were analyzed by scanning electron microscopy (SEM) for investigation of the surface morphology changes and by Electron Dispersive X-ray Microanalysis (EDX) for determination of the elemental composition. The EDX spectra have been analyzed by a standardless ZAF correction method. The penetration depth of the electrons and the spatial distribution of the X-rays have been assessed with the Monte–Carlo code CASINO by taking into account the microscope beam conditions. About 90% of the signal produced originates from a depth less than 1 μm, much less than the size of the reprecipitated phases. The powdered phases used in the third set were analyzed by X-ray diffractometry.

2. Experimental

2.1. Leaching experiments

UO_2 alteration processes were investigated with anoxic leaching experiments using groundwater with step-

wise enhanced content (10^{-4} to 10^{-2} mol/l) of the ions SiO_2 (aq), Ca^{2+}, and CO_3^{2-}. A natural, commercially available groundwater was spiked with solutions of $CaCl_2$, $NaHCO_3$ and Na_2SiO_3 and contacted with pellets of UO_2 under argon atmosphere (<2 ppm O_2). Dilution of Na metasilicate solutions was found to result in the formation of mainly monomeric Si species at pH 9–10 [14] which do not polymerize up to concentrations of 12 mmol. Since the dominant Si species in solution at pH 7.5 is monosilicic acid ($Si(OH)_4$), whereas at pH 9 it is $H_3SiO_4^-$, we assign the general term 'SiO_2 (aq)' for dissolved Si in our experiments in the following. Two sets of experiments were conducted: one at ambient conditions (25 °C, atmospheric pressure), the second at hydrothermal T and p conditions (180 °C, enhanced pressure) in stainless steel autoclaves using teflon liners as reaction vessels. The pH values and redox potentials of the tests conducted at ambient conditions were measured prior and after the experiment. The pressures of the reacting solutions were not measured; they can be assumed to be approximately equal to the vapor pressure of water at the given temperatures (e.g., 1.5 MPa at 200 °C).

2.2. Materials

Pellets of nuclear-grade depleted UO_2 with an approximate weight of 1.2 g were used as solid phase in the leaching experiments. Composition and purity of the material was checked by ICP–MS analysis, showing that Ba, Sr and Mo were present in detectable concentratios. Fe, Ti or Ni were not found. The values are given in Table 1. The specific surface area, not directly measured, was assumed to be $1.9 \times 10^{-4}\ m^2 g^{-1}$ after the compilation data referred by Oversby [15]. The initial roughness in the pellet surface structure promotes local nucleation of solid precipitates during the leaching experiments [16].

Before each experiment, the samples were annealed for 5 h at 1600 °C in an Ar/H_2 atmosphere (96:4, both gases with a max. impurity of 5 ppm oxygen) in order to restore the stoichiometry of pure UO_2 as far as possible and to rule out the participation of U^{6+} ions in the leaching process from the beginning.

Table 1
Elemental analysis of the UO_2 material used for the experiments

Element	Content (wt%)
Sr	0.0015
Ba	0.038
Mo	0.0047
Fe	–
Ti	–
Al	–
Zr	–
Ce	–
U	99.9558

Values relate to a total metal content of 100%. Elements for which no value is given were measured to be present in concentrations below the detection limit of ICP–MS.

Table 2
Concentration values of several ions present in groundwater, measured for an anoxic (degassed) sample at pH = 7.4

Ion	Content (mol/l)
Na^+	5.05×10^{-4}
K^+	1.74×10^{-4}
Mg^{2+}	2.94×10^{-4}
Ca^{2+}	2.72×10^{-4}
Fe (total)	1.97×10^{-5}
U (total)	2.32×10^{-9}
Al^{3+}	3.00×10^{-9}
Ti	2.06×10^{-7}
Cl^-	3.53×10^{-4}
NO_3^-	8.50×10^{-5}
SO_4^{2-}	8.15×10^{-5}
HCO_3^-	1.68×10^{-3}
F^-	1.40×10^{-5}
SiO_2	4.99×10^{-4}
PO_4^{3-}	1.04×10^{-7}

A natural groundwater was used as contacting liquid phase. The ionic composition was determined by the Institute of Petrography and Geochemistry (IPG) of the University Karlsruhe with inductively-coupled-plasma mass spectrometry (ICP–MS) for heavy metal ion detection, atomic absorption spectrometry (AAS) for light element detection and ion chromatography (IC) and photometry for anion detection. The ionic composition of the groundwater is given in Table 2.

In order to check the overall redox behaviour, a groundwater sample was degassed with Ar (having a max. impurity of ca. 2 ppm) for ca. 36 h. A decrease of Eh values is observed immediately after start of the degassing procedure. After 100 min, negative Eh values are reached. An additional measurement with an Au redox electrode was performed to cross-check the procedure. After ca. 1200 min, an Eh plateau is reached and for the rest of the degassing procedure the values oscillate around −180 mV versus the standard hydrogen electrode (shown in Fig. 2). During the purging procedure the content of dissolved O_2 was monitored using a WTW CellOx 325 sensor. When Eh values below −100 mV were measured, the O_2 content dropped below the detection limit of the system (<0.05 mg/l) and remained undetectable throughout the rest of the procedure.

2.3. Methods

Extreme care was taken to ensure oxygen-free environments for the duration of the leaching tests. An overpressure inert gas glovebox was used through which Ar

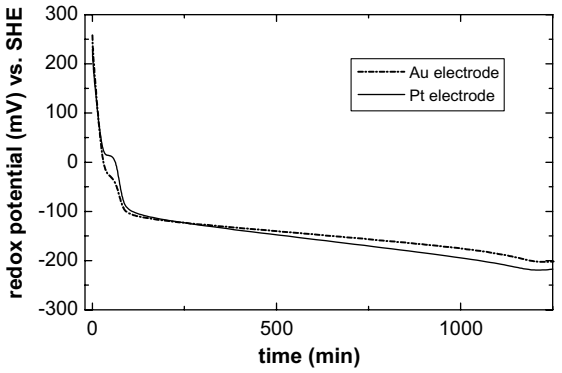

Fig. 2. Development of the redox potential (versus SHE) in groundwater during degassing to anoxic conditions (purging with Ar), measured with Pt and Au electrode.

was purged with a starting O_2 content of <2 ppm. The Ar was further purified by a double chromatography oxygen trap (Agilent). Scintillation vials (20 ml volume) were used for the leaching experiments at ambient temperature conditions. A volume of 10 ml solution (groundwater) was contacted with a pellet of UO_2. The resulting m/V-ratio of about 1.2/10 gcm^{-3}, which is relatively high for this type of experiments, was chosen to facilitate the formation of secondary alteration phases on the sample surface. An overview about the use of m/V-ratios for different experiments is given by Loida and coworkers [17]. Eh values of the solutions reacting at ambient temperatures were monitored prior and after the tests. A Mettler Toledo 4805 Pt/Au electrode together with a WTW Multilab P 5 measurement unit were used for redox control. The O_2 content in the inert gas was monitored continuously with an oxygen sensor (Orbisphere). The Eh values of the solutions reacting at enhanced temperatures could not be monitored since the vessels' interior was not accessible for the electrode prior to phase separation (however, a blank test using groundwater without a solid phase or additive was measured after treatment at 180 °C and, resulting in an Eh value of −8 mV).

During 1000 h, the samples were agitated at regular intervals. At the end of the contacting time, liquid and solid phases were separated, liquids were filtered with 450 nm filters. Solid phases were rinsed with a small volume of distilled water to remove adjacent particles and dried in argon atmosphere. Solutions were stored until bulk solution elemental analysis was performed with ICP–MS.

The experimental set done under hydrothermal conditions was treated identically except that teflon liners of 40 ml volume were used as reaction vessels, which were sealed and heated to 180 °C in a steel bomb autoclave for the duration of the experiment. Prior to sampling, the system was cooled down slowly to room temperature and equilibrated for additional 96 h, thereby assuming that element concentrations were in equilibrium with possible newly formed phases, instead of measuring high-temperature solubilities. The third set of experiments is abbreviated ISDP ('infinite ion supply by dissolving phases') in the following. About 0.3 g of analytical-grade CaO, TiO_2, and a mixture of metallic Fe and Fe_2O_3 were sealed with quartz frits and quartz wool in quartz micro vials. The vials were placed, together either with a UO_2 pellet, or 1 g of powdered UO_2 material, in spiked groundwater solution ($[Si]_{diss} = 10^{-2}$ mol/l) in anoxic atmosphere, and subsequently heated to 180 °C for 100 days. Two tests were also made without the phases present (only UO_2 in aqueous medium, $[Si]_{diss} = 10^{-2}$ mol/l). After ending the experiment, solutions were analysed with ICP–MS for element concentrations and the solids were investigated with SEM–EDX. The set-up of ISDP is shown in Fig. 3.

Preparation, conduction and phase separation took place under argon atmosphere at ca. 2 ppm oxygen. All vessels were conditioned for 5 days with 0.1 M HNO_3 and equilibrated with groundwater for 5 days prior to the conduction of the experiments.

In each case a blank test (UO_2 and untreated groundwater) was run to investigate the behaviour of the system without ion addition to the solution. Additionally, the natural U content of the groundwater was measured before the water had contact with the UO_2 samples.

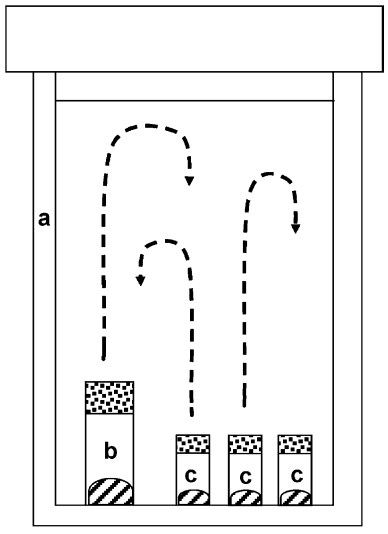

Fig. 3. Experimental set-up of the hydrothermal UO_2 leaching experiment in presence of dissolving phases ('ISDP experiment'): (a) teflon reaction vessel heated to 180 °C; (b) quartz vial containing UO_2; (c) quartz vials containing TiO_2, CaO, Fe_2O_3/FeO; (d) natural groundwater ($E_H = -280$ mV, $[O_2]$ <0.05 mg/l), 0.01 mol/l SiO_2 (aq) were added).

2.4. Bulk solution analysis of the samples and solution geochemical parameters

After terminating the experiments, solid and liquid phases were separated by filtration through 0.2-μm filters. The leachates were analysed for uranium concentration with inductively coupled plasma mass spectrometry (ICP–MS). The solution geochemical boundary parameters pH, Eh, and [Ca^{2+}] were determined according to the procedures described above. The results are compiled in Table 3.

2.5. Determination of U oxidation state

It was attempted to determine the oxidation state distribution of uranium in four samples (those containing 10^{-2} mol/l of the additives at ambient temperature) by adapting the procedure described by Fattahi and Guillaumont [18]. A volume of 10 ml of the leaching solution was mixed with concentrated HCl (9 M, suprapur grade, Merck) in order to ensure Cl^- complexation of U in solution. U(IV) is known to form cationic complexes with Cl^-, whereas U(VI) was reported by the mentioned authors to form anionic chloro complexes; however, data compiled in the NEA thermodynamic database [19] suggest that U(VI) complexation with Cl^- proceeds to the neutral complex only. This discrepancy and its consequences will be discussed further below. The resulting solution was passed over a column filled with Dowex 1 anion exchange resin, collected, and analyzed for U content with ICP–MS. This fraction contains the fraction of U present as U(IV). Subsequently, the exchanger column was eluted with 10 ml of 0.1 M HCl in order to mobilize the U(VI) fraction. The eluent was collected and analyzed with ICP–MS.

2.6. SEM–EDX

The solid phases were rinsed with a small volume of deionized water to remove residuals of the leaching solutions and afterwards dried for 7 days in a mild vacuum. Examination with SEM–EDX was performed with a Philips SEM 515 scanning electron microscope at an acceleration voltage of 25 kV, using a Tracor detector for the EDX measurements. Samples were placed on an aluminium cup sample holder and, thanks to the sufficiently high electrical conduction of UO_2, needed no noble metal coating. The electron beam generates signals coming from a spherical volume element in the solid matrix; EDX analysis is therefore prone to deliver signals from the underlying substrate if the objects measured are sufficiently small. In such a case, a quantitative evaluation becomes impossible. In order to assess the situation in our case we calculated the penetration depth using the EDX simulation code CASINO [20]. It proved that for the parameters used (acceleration voltage, substrate material, and geometry), signals coming from depths greater than 1 μm contribute to about 10% of the uranium signal evaluated. Considered that most objects measured in this study are larger than 1 μm, the measured spectra are expected to contain no uranium artefacts.

3. Results and observations

3.1. Leaching of UO_2 in groundwaters with altered composition – ambient temperature conditions (25 °C)

$[U]_{diss}$ for the experiments performed under ambient conditions are shown in Fig. 4(a). The change in the ionic composition of the leaching groundwater was found to have an effect upon $[U]_{diss}$ in some cases.

Dissolved uranium concentrations were found to be minimally influenced when small quantities of the spiking are added (10^{-4} mol/l). However, when additives are present in the groundwater at 10^{-2} mol/l, $[U]_{diss}$ are altered, particularly significant in the case when applying the 10^{-2} mol/l SiO_2 (aq) spiking. In this case the addition results in noticeable decrease of $[U]_{diss}$.

Table 3
Shift of pH and [Ca^{2+}] during leaching of UO_2 at ambient temperature (T = 25 °C)

Conditions in experiment	pH (t = 0)	pH (t = 1000 h)	[Ca^{2+}] after 1000 h (25 °C)	[Ca^{2+}] after 1000 h (180 °C)
Groundwater (GW), unspiked	7.54	9.10	1.25×10^{-7}	1.37×10^{-5}
GW + [Ca^{2+}] = 10^{-4} M	7.40	–	1.25×10^{-7}	1.84×10^{-5}
GW + [Ca^{2+}] = 10^{-3} M	7.23	9.03	1.25×10^{-7}	2.86×10^{-4}
GW + [Ca^{2+}] = 10^{-2} M	7.08	8.80	1.60×10^{-6}	2.82×10^{-4}
GW + [CO_3^{2-}] = 10^{-4} M	7.48	9.35	1.25×10^{-7}	3.03×10^{-5}
GW + [CO_3^{2-}] = 10^{-3} M	8.10	9.43	2.74×10^{-7}	9.41×10^{-6}
GW + [CO_3^{2-}] = 10^{-2} M	9.75	9.63	1.25×10^{-7}	5.77×10^{-6}
GW + [SiO_2 (aq)] = 10^{-4} M	7.37	9.10	3.74×10^{-7}	3.61×10^{-6}
GW + [SiO_2 (aq)] = 10^{-3} M	9.09	9.27	1.25×10^{-7}	2.58×10^{-7}
GW + [SiO_2 (aq)] = 10^{-2} M	10.00	10.29	1.25×10^{-7}	2.76×10^{-5}

The pH was measured prior and after the tests. Ca concentrations were measured after 1000 h and several days of equilibration. For comparison, Ca concentrations after the 180 °C experiments are also given.

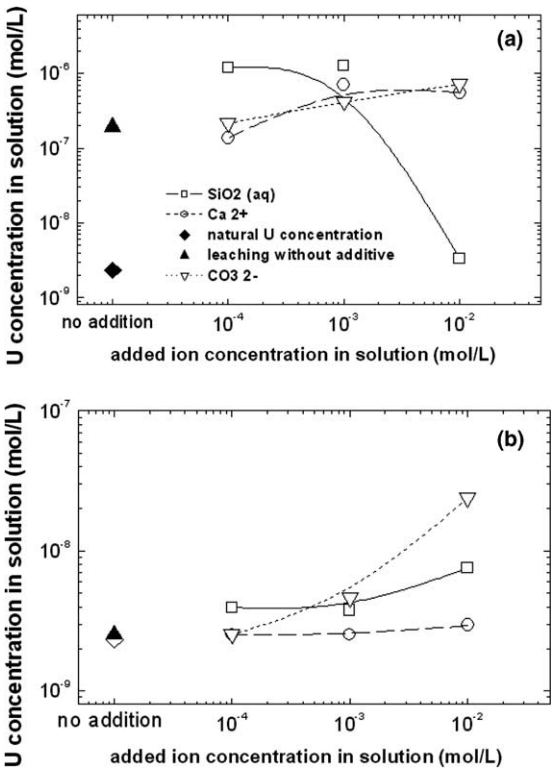

Fig. 4. U concentrations after UO_2 leaching at (a) 25 °C (ambient conditions) and at (b) 180 °C (hydrothermal condition) for 1000 h in altered groundwater under anoxic atmosphere. The single points show the natural U content in the water (rhomb) and the U concentration after leaching with unaltered groundwater (triangle).

Carbonate addition to the groundwater results in a slow and constant increase of $[U]_{diss}$ with increasing amount of carbonate added. Addition of Ca^{2+} gives first an increase, then a decrease of the mobile uranium fraction in the system, lacking a clear trend.

The leaching of UO_2 with unspiked groundwater results in a value of 1.94×10^{-7} mol/l U in solution concentration which is in good agreement with measurements by other authors at near neutral pH and ambient temperatures (e.g., [21]). Since solubility data depend often on the physical shape of the solid phase (powder, monoliths, etc.), it is difficult to state if the material used in this investigation did slightly oxidize immediately before the experiment was started, or if insufficient filter pore size allowed the passing of particulate matter (e.g., colloids) into the measured solutions. In the examples discussed here, we consider the second case most possible, since 0.2 μm filter cannot guarantee the complete exclusion of fine particles.

The pH–Eh monitoring shows that after terminating the experiment, pH values have shifted notably, whereas redox potentials of the liquid phases are well within the anoxic region (between −69 and −186 mV versus SHE). For some of the experiments, the Eh values increased whereas with others, lower values were found, thus lacking a clear trend. Generally, pH values were measured to be higher than compared with the beginning of the tests. We conclude that this is due to the purging procedure of the reacting fluid with Ar, during which CO_2 contained in the fluid is removed. Usually this process raises the pH (as described in [22] or [23]) and leads to calcite precipitation. The change of $[Ca^{2+}]$ can be seen also from the values given in Table 3, which were measured after the tests. Since calcite precipitation is usually kinetically slow, the effect was not visible at $t = 0$ (at the first pH measurements).

The results of the ion exchange procedure, which was used for the separation of the U oxidation states +VI and +IV, are compiled in Table 4. The solutions resulting from the experiments with addition of the three additives in the highest concentration (10^{-2} mol/l), as well as the solution of the experiment performed with unchanged groundwater, were investigated. The sample resulting from non-spiked groundwater results in the lowest content of U(IV) (about 18%). The highest content of U(IV) is found for the sample having an enhanced concentration of carbonate (37%), the values for the remaining samples are inbetween these two values. The results suggest that a significant portion of U is present in the U(IV) state, but, however, the majority of uranium ions in the bulk solution are present as U(VI). The results of an oxidation state separation procedure performed by Ollila [24] for a similar experimental setup, but conducted under a N_2 atmosphere containing 10% of H_2, showed slightly higher percentages of U(IV) (e.g., 37% after 56 days of leaching). Thus, even under strongly reducing experimental conditions, a partial oxidation of dissolved U is difficult to avoid. The results of this procedure need to be interpreted with some care. As mentioned, it is so far not clear if U(VI) complexation will only proceed until the neutral chloro complex (as selected by the NEA [19]) or if it may include the formation of negatively charged complexes (as suggested in [25]). We calculated theoretical E_H values that correspond to the measured U(VI)–U(IV) ratios; these demonstrate that for the pH-neutral solutions (pure and Ca added), actual ratios should in fact have a higher fraction of U(IV) whereas for the alkaline systems, U(VI) should in fact prevail. Due to this pH-dependence of the oxidation state, the results of our separation should be considered as a first indication.

The analysis of the naturally abundant U content in the groundwater gave a value of 2.32×10^{-9} mol/l, which is in good agreement with the results found for other typical groundwaters [26]. We took into account this background value when evaluating uranium concentration coming from the UO_2 dissolution, but generally these were higher.

Table 4
Measured ratios of the uranium redox states +IV and +VI after the leaching experiment at ambient temperature in the samples spiked with highest additive concentrations (10^{-2} mol/l), as well as for unchanged groundwater

Experiment	Ratio U(IV)/U(VI) (experimentally determined)	Corresponding Eh (by thermodynamic calculation)[a]
Pure	0.17:0.83	+41
10^{-2} mol/l Ca^{2+} added	0.25:0.75	+35
10^{-2} mol/l CO_3^{2} added	0.32:0.68	−305
10^{-2} mol/l SiO_2 (aq) added	0.27:0.73	−266

In the second column the corresponding Eh values (mV) are given, as determined by geochemical equilibrium calculation.
[a] Calculated using the code PHREEQC V 2.6 and the NEA database [19].

3.2. Leaching of UO_2 in groundwaters with altered composition – hydrothermal temperature conditions (180 °C)

After hydrothermal treatment, lower U concentrations were measured in the leachates (about 10^{-9} mol/l U) for samples containing low additive concentrations (Fig. 4(b)). At higher additive contents, U concentrations rise for about one order of magnitude. No decrease of U concentration with enhanced solution ion content was observed, as found for the ambient conditions case.

3.3. Surface analysis of the solid phases and SEM–EDX results

The pellets and powders used as the solid phase in the experiments were examined visually and subsequently the surfaces were inspected by scanning electron microscopy in order to detect surface modifications.

Samples treated at ambient conditions (at 25 °C) showed no changes in the surface structure compared to an unleached sample. The only difference was that many micrometer-sized particles were found to be scattered over the surface, which might be due to fines generated during the dissolution process and accumulated on the surface. These particles were found to contain U as only element. Genuine surface phase crystallisation could not be observed for none of the four experiments and no evidence for structures with a crystal shape resembling to that of schoepite ($UO_2(OH)_2 \cdot nH_2O$), or other U(VI) mineral phases, could be found. Schoepite is usually found on UO_2 surfaces after leaching treatment under oxic conditions [27].

In contrast, the surface of all four samples treated at hydrothermal conditions was considerably altered and damaged. The visual inspection showed for the specimen contacted with carbonate ions a grey-white discolouration on the surface, whereas the one contacted with silicate solution showed a blue-grey discoloration. SEM investigation revealed, as a common observation, the preferential etching at grain boundaries and gap widening between grains. The surface of the UO_2 sample exposed to 10^{-2} mol/l Cl^- displayed cavities and holes most clearly. The samples treated with carbonate and silicate were less damaged but frequently areas of different grey shades in the SEM image were detected, indicating a layer formed on the surface. Samples treated in Si-enriched solutions were the only ones that displayed cracks.

The surfaces of the hydrothermally treated specimens were measured with EDX in order to analyze the composition of a layer or secondary phase possibly formed. In the case of the samples treated with additives at 10^{-3} and 10^{-4} mol/l as well as in pure groundwater, only U was detected. The sample treated with groundwater containing 10^{-2} mol/l SiO_2 (aq) showed patch-like black fields in the SEM image which cover about 1/4 of the whole sample surface. The grain boundary structure of the material is notably damaged and cracked within these domains, and here EDX examination found a high Si content. U and Si were repeatedly measured with a ratio close to 1:1. No uranyl mineral matching this ratio having only U and Si as constituents could be identified. Presumably synthetic coffinite ($USiO_4 \cdot nH_2O$) has formed during the experiment. In order to collect more information on the spatial distribution of the Si enrichment on the surface, an EDX line scan across the Si-enriched zone was performed. It shows a depletion in U and, at some locations, the presence of minor Mg, as shown in Fig. 5(b). A quantitative analysis of the elemental composition at the locations investigated was performed with the EDX technique, the results are shown in Table 5.

Further crystalline structures with a diameter of about 10 μm were detected on the surface of this sample. The EDX analysis showed that Fe, Ca, U, and Si and Ti are present in these objects. The crystals did not appear together with the Si-enriched areas and were observed rarely on the whole sample surface, however always a typical radial shape and a similar elemental composition were observed. This suggests that a mineral phase with a constant composition was formed. The phase was not found in the other hydrothermal experiments. Fig. 5(a) displays a SEM micrograph and the EDX spectrum

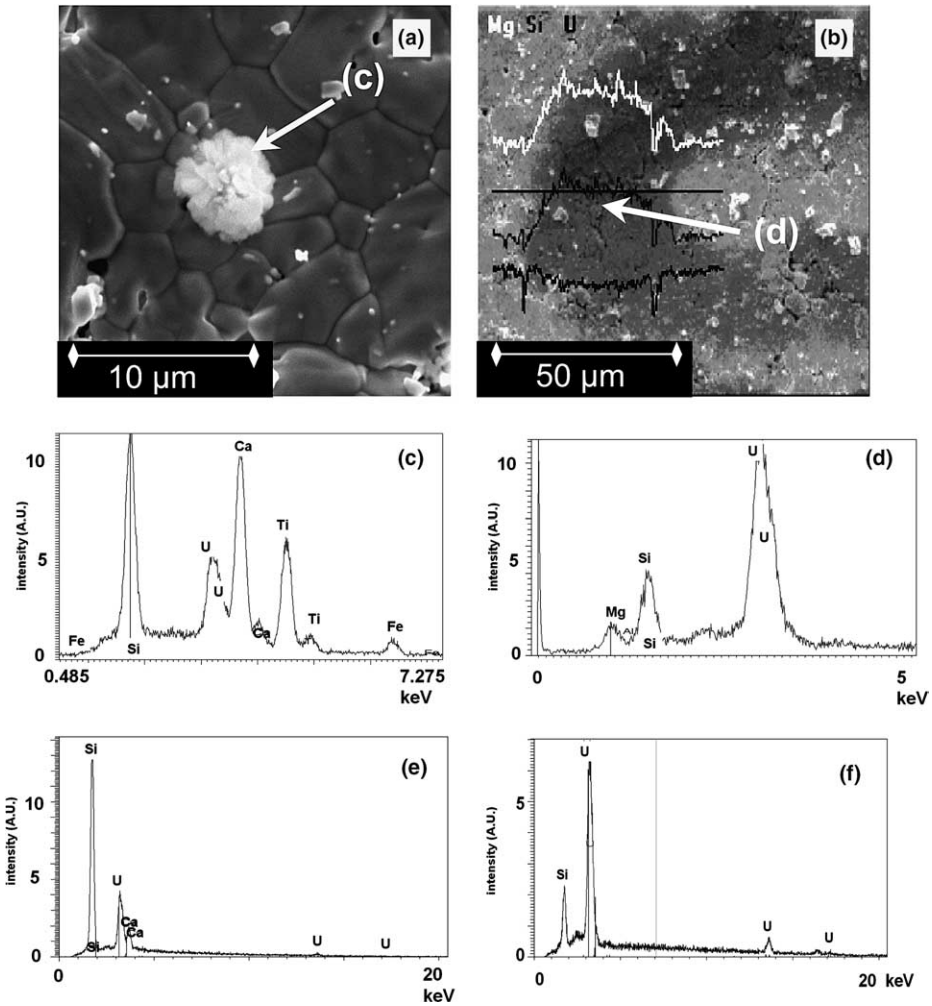

Fig. 5. SEM images and EDX spectra taken from a UO_2 sample leached at 180 °C in groundwater containing a Si concentration of 10^{-2} mol/l. (a) SEM image of an alteration phase found on the UO_2 sample leached at 180 °C in groundwater containing a Si concentration of 10^{-2} mol/l. (b) SEM image of a zone enriched in Si and EDX line-scan profile for the elements U, Si, and Mg, measured across a discolouration zone found on the SEM image. The measurement shows a depletion of U and the presence of Si and Mg in the dark zone. (c) EDX spectrum of the phase shown in (a), showing the elements U, Si, Ca, Ti and Fe present. (d) EDX spectrum of U–Si phases with irregular stoichiometry. (e) EDX spectrum of the U–Ca–Si phase (ratio 1:2:8) generated in the ISDP experiment. (f) EDX spectrum of a U–Si phase with the elements ratio 1:1.

Table 5
Element contents (at.%, normalized to U values) of the observed secondary phases

Phase formed on UO_2 (observed in this work)	U	Si	Ca	Mg	Fe	Ti	O calculated (see text for explanation)
U–Si (–O)	1	1.03	–	–	–	–	4
U–Si–Mg (–O)	1	0.86	–	0.27	–	–	4
U–Ca–Si (–O)	1	7.65	1.89	–	–	–	20
U–Ca–Fe–Ti–Si (–O)	1	7.06	6.58	–	0.48	4.18	38.5

measured from these objects. The elemental composition derived from the spectra was compared with those reported for samples of the minerals ekanite [28,29], brannerite [30], davidite [31], and chevkinite [32] (see Table 6 for formulas). These minerals can bear a significant amount of U(IV) within their structure. The results

Table 6
Minerals containing U(IV) and, partially, other elements present in the water used in this work

Mineral	Formula	Ref.
Coffinite	$U(SiO_4)_{1-x}(OH)_{4x}$	[53]
Non-stoichiometric U–Si phase	$(U^{4+}, U^{6+})_2SiO_6$	[43]
Brannerite	$(U,Ca,Ce,Y)[(Ti,Fe)_2O_6]$	[30]
Ekanite	$(Th,U)(Ca,Fe)_2Si_8O_{20}$	[28,29]
Steacyite	$(Th,U)(Na,Ca)_2(K_{1-z}\square_z)Si_8O_{20}$	[69]
Chevkinite	$(Th,Ca,La,Ce)_4Fe^{2+}(Ti,Fe^{2+/3+})_2(Ti)_2Si_4O_{22}$	[32]
Davidite	$(La,Ce)(U,Y,Fe)(Ti,Fe)_{20}(O,OH)_{38}$	[31]
Ca-Betafite	$(Ca,U,Th)_2(Ti,Nb)_2O_7$	[42]
Calciosamarskite	$(Ca,Fe^{3+}\ U,Y)(Nb,Ta)O_4$	[70]

Some are suspected to possibly form as secondary phases in anoxic UO_2 alteration experiments.

of the EDX analysis for the phases found in this work are compiled in Table 6. The composition reported for some samples of chevkinite match well with the phases observed in our experiments, as will be discussed below.

In an attempt to investigate the nature and structure of this compounds, a further hydrothermal experiment was performed, during which dissolving UO_2 (as pellets and powdered) was placed in anoxic hydrothermal solution together with analytical grade TiO_2, Fe(0), Fe_2O_3, CaO, and SiO_2 (shown in Fig. 3). In parallel, the hydrothermal leaching treatment with groundwater/10^{-2} M Si (no further solid phase present) was repeated for both pellets and UO_2 powders, in order to obtain a more complete reaction due to enhanced active surface, and to enable powder XRD analysis. In the following, this experiment is abbreviated with 'ISDP' ('infinite ion supply by dissolving phases'). The UO_2 surface showed macroscopically a blueish colour after this treatment and EDX measurements found the elements U, Ca, and Si to be present in the ratio 1:2:8. This ratio is not found with any known U(VI) mineral. However, the Th minerals of the ekanite group contain Th, Ca, and Si in this ratio so that a U-ekanite might have resulted from the experiment, as will be discussed below. The phase containing U, Ca, Si, Fe, and Ti observed after the experiment in groundwater / 10^{-2} M Si, was not found here. Solution analysis was done by ICP–MS for all four solutions. The results are compiled in Table 7. XRD measurements were taken from both powdered materials leached in the presence and without the additional phases, shown in Fig. 6. Furthermore a sample of unleached material was measured. The diffraction patterns analysed by a Rietveld-type profile refinement method revealed nothing else but pure stoichiometric UO_2 with $a = (547.05 \pm 0.02)$ pm in the unleached sample. After hydrothermal leaching, all diffraction UO_2 peaks are

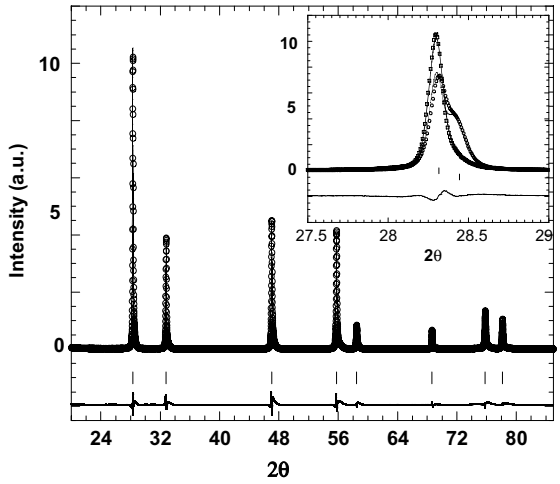

Fig. 6. X-ray powder diffraction pattern of the UO_2 sample material, before and after the experiment. The symbols represent the observed points, the solid lines represent the calculated profile and the difference between observed and calculated profiles. The ticks correspond to $2\theta_{hkl}$ Bragg positions of the phase. The inset shows a zoom around the (111) UO_2 diffraction peaks before (square) and after (round) the ISDP hydrothermal experiment.

Table 7
Concentrations (in mol/l) of Ca, Fe, Ti, and U in the leaching solutions after the four tests of the ISDP experiment

Conditions in experiment (state of UO_2/c (Si))	Concentration of element in solution (mol/l)			
	U	Ca	Fe	Ti
Pellet/[Si] = 10^{-2} M	4.55×10^{-8}	1.92×10^{-4}	1.06×10^{-6}	1.05×10^{-7}
Powder/[Si] = 10^{-2} M	1.75×10^{-7}	1.20×10^{-5}	6.09×10^{-7}	2.86×10^{-7}
Pellet + dissolving solids/[Si] = 10^{-2} M	1.48×10^{-8}	8.53×10^{-5}	1.92×10^{-5}	7.56×10^{-7}
Powder + dissolving solids/[Si] = 10^{-2} M	2.03×10^{-8}	1.66×10^{-5}	4.19×10^{-7}	7.69×10^{-8}

split into two different peaks with distinct intensity. The highest peaks still correspond to UO_2 with unit cell parameters identical with those determined in the unleached materials. These additional signals, displayed in the insert of Fig. 6, indicate that keeping the UO_2 structure, part of the UO_2 reacts. The strong decrease of the unit cell parameters $a = (544.61 \pm 0.03)$ pm might be due to the intercalation or to the formation of solid-solution like $U_{1-x}R_xO_2$. Furthermore, careful analyses of the powder pattern thus obtained indicate the presence of weak additional signals that could be attributed to a coffinite-like structure [33], although the highest intense peak is missing. No signals that indicate the presence of further phases were found, proving that UO_2 is the only well-crystallised material present in the sample.

4. Discussion

4.1. Concentration profiles and surface alterations under ambient conditions (25 °C)

The variation of Ca concentration in the leaching solutions obviously led to little effect upon the U solubility, as was observed both with the experiments under ambient and hydrothermal treatment. A possible incorporation [34] or coprecipitation mechanism, in which both Ca and U are involved, seems to play a minor role in the variation of U concentrations in this experiment. Curti [11] found a strong impact of calcium chemistry upon the solubility of U(IV) which is controlled by coprecipitation of the latter with calcite. Therefore, the pH conditions of geochemical stability necessary for calcite precipitation out of low-ionic strength solutions need to be reached [35,36], which was not the case in the experiments in this work (pH values of about 7 were measured for the tests with Ca).

Slightly enhanced UO_2 dissolution was observed in both experimental sets when higher carbonate concentrations were used. Carbonate is known to act as a strong complexant for uranyl ions in aerated conditions; in the case of U(IV), the formation constants for U-carbonato complexes (as stated in Fig. 1) are low enough to consider their contribution to the dissolution process as insignificant [37,38]. The observation of carbonate-enhanced uranium dissolution in anoxic environments was also explained by an electron transfer mechanism during which the carbonate ion possibly initiates the formation of uranyl ions from a U(IV) matrix (reviewed in [12]). However, we have no evidence for such reactions having taken place in the systems investigated in this work.

The concentration decrease observed in the case of SiO_2 (aq) addition is probably due to a surface sorption and/or partly precipitation of a solid formed in the solution. It was not observed when the experiment was performed at hydrothermal conditions; in this case, higher Si concentrations favoured a higher U solubility. According to Fuchs and Hoekstra [39], the formation of U(IV)silicate (coffinite, $USiO_4 \cdot nH_2O$) at room temperature can be ruled out within laboratory experiment timescales (weeks or months). SiO_2 has probably formed (e.g., as a thin layer) and precipitated U at room temperatures; this could not be proved. About the solubility characteristics of coffinite at higher temperatures, only insufficient facts are known.

4.2. Concentration profiles and surface alterations under hydrothermal conditions (180 °C)

The considerably lower U concentrations measured after the hydrothermal experiment are in accordance with the results of earlier measurements of UO_2 solubility in elevated temperature conditions [40] and with those obtained from studies conducted in alkaline solutions [41]. In the present case, samples were taken from the system after its return into a state that was assumed to be in thermodynamic equilibrium with ambient conditions ($p = 100$ kPa, $T = 25$ °C); therefore, the concentration profiles must be seen in the view of the chemistry of the solid phases present at these conditions, which will be discussed later.

The interesting surface alterations (from a chemical point of view) that were discovered on the hydrothermally leached samples, occur on the specimen exposed to a solution containing $[Si]_{diss} = 10^{-2}$ mol/l (Fig. 5). Areas with a high (about 50 at.%) Si content were measured; the U–Si ratios were almost constantly 1:1 at most locations. The product resulting from a synthesis described in [42] (performed in the presence of powdered UO_2 in freshly precipitated 1.5-molar SiO_2 suspension) delivered a nearly identical EDX spectrum. No distinct crystal structure could be observed in both cases. Therefore the XRD analysis did not convincingly prove the presence of $USiO_4 \cdot nH_2O$. In addition, precipitated Si was found in other areas of the surface in minor quantities. The EDX analysis then gave results of 90–100 at.% Si. In natural coffinite-containing samples, a wide variety of U–Si ratios can be found. In coffinite from the West Balkan metalogenic zone (Bulgaria), a U–Si ratio between 2:1 and 1:1 was determined [43]. Here, equally, no defined crystals were identified. Since coffinite is known to form at hydrothermal conditions in nature [44], and since it was possible to synthesize it under laboratory conditions [45,46], its formation during our experiments seems plausible. The observation that the macroscopic structure of the leached UO_2 material is changed (visible as cracks where a high abundance of Si was detected on the surface) supports the assumption of phase transformation. During the hydrothermal reaction of SiO_2 with UO_2 a change of the crystal lattice from the fluorite-type (UO_2) to the zircon-type (coffinite)

occurs, macroscopically visible as damage in natural samples [47,48]. However, we cannot explain why the formation of the described phase took place only on certain parts of the surface. Preferential nucleation induced by surface roughness or lattice effects might play a role [16].

In addition to the proved U/Si ratios of about 1:1 in the investigated areas, minor quantities of Mg were found to be included in few measured locations. Such trace components were also observed in natural coffinite. Fig. 5 shows the presence of Mg during a line scan across the Si-enriched zone visible as dark field in the SEM image.

The compound containing U, Ca, Si, Ti and Fe – we assume O to be present, although it was not determined – that was found on the sample treated in 10^{-2} mol/l silicate solution, seems to be a separate crystalline structure rather than a layer. Considering the relatively low Fe content of the groundwater (in the order of 10^{-5} mol/l), the formation of a Fe-containing secondary phase was not expected. The observed substance is probably identical with or, at least, related to a naturally occurring mineral phase. Since the compound did not form in solutions containing a low Si concentration ($<10^{-2}$ mol/l), Si is assumed to be an essential for its formation. Compounds with an elemental composition of interest are the minerals of the chevkinite group ($A_4BC_2D_2Si_4O_{22}$, with A = REE, Ca, Sr, Th,U; B = Fe^{2+}; C = Ti, Al, Fe^{3+}, Fe^{2+}; and D = Ti) [32], ekanite ($(Th,U)Ca_2Si_8O_{20}$) [29], brannerite ($(U,Ca,Ce)(Ti,Fe)_2O_6$) [30], calciobetafite ($(Ca,U,Th)_2(Ti,Nb)_2O_7$) [48], and davidite ($(La,Ce)(U,Y,Fe)(Ti,Fe)_{20}(O,OH)_{38}$) [31], with alternating content of trace elements depending from their genesis. In the case of ekanite, the presence of U is of accessory nature and the element is not essential for the crystal structure of the substance; however, it is assumed that U and Th can freely substitute for each other [9]. In the case of brannerite, some of the elements found in the analysis here are not present in the mineral in its pure state, but are often found associated with the phase [30,49]. The measured element ratios were normalised on U content (compiled in Table 5) in order to allow comparison with the reported mineral formulas (compiled in Table 6). The O contents given in Table 5 were calculated from the phase formulas using the data measured for the other elements. On none of the sample surfaces examined, structures known from U(VI)-minerals were observed, e.g., schoepite, uranophane, or soddyite.

4.3. Phases found after the ISDP (infinite ion supply by dissolving phases) experiment

After ending the treatment, UO_2 surfaces had blue discolorations and SEM investigation revealed three separate areas containing crystalline objects of different shape. Within the largest of the areas, a compound with nearly constant compositional ratio of U/Ca/Si = 1:2:8 was measured. Measurements in the other fields resulted in U/Si = 1:1, or contained principally Si. No Ti or Fe was incorporated into the product.

Of the dissolved elements concentrations, only $[U]_{diss}$ showed a dependence on changing the chemical environment in solution. Concentrations were found to be about one order of magnitude lower when additional dissolving phases were present. It is remarkable that the enhanced surface area of UO_2 powder had almost no effect on $[U]_{diss}$ in the experiments performed in the presence of solid phases. In the other tests, in absence of the additional phases, using powdered UO_2 results in values about one order of magnitude higher, which might be due to fine particles not separated by the filtration procedure. In the case of phases present, these particles were possibly converted, together with the greatest part of the surface of UO_2, to a secondary compound with a solubility different to that of UO_2.

4.4. Discussion on potential U(IV) secondary phases

Several of the U(IV) minerals mentioned in Table 6 can be generated hydrothermally (both by nature and synthesis) [50,51]. Brannerite and ekanite were reported to appear in hydrothermal and sedimentary deposits. In the case of brannerite, the presence of Ti is essential for formation since TiO_6 units form the framework of the structure which is filled with interstitial U and Ca [9]. However, the high Si content of the U–Si–Ca–Fe–Ti phase shown in Fig. 5(a) suggests brannerite formation as unlikely. The formula of ekanite does not match with the ratio of elements observed for the discovered phase. The mineral betafite (a member of the pyrochlore group) also seems to be less probable to explain the observations, since it is generated by magmatic processes. It was found that minerals of the betafite group can gain Fe during hydrothermal alteration [52]; also a certain Ca content was found when the element substitutes U on the A positions. However, since these phases do not contain significant Si amounts they are not considered further. Chevkinite group minerals are the only phases with a composition that would match what we did observe by EDX measurements.

Coffinite was first described as an independent mineral phase in 1956 [45,53] and is reported with a composition of $USiO_4 \cdot nH_2O$. This matches well with the constant ratio U–Si of 1:1 observed with one of the phases. The fact that a penetration of Si into the host matrix will change the lattice structure and cause defects leading to its destruction is of great importance for the stability of the host structure in the presence of Si (and hence for the solubility of the material also). Coffinite was observed to suffer from the attack of oxygenated water in a similar manner as UO_2 [7].

The observed ratio of the elements identified in the ISDP experiment products does not coincide with the composition of any known uranyl phase [54]; however, it matches the composition of the Th/U(IV) mineral ekanite ($(Th,U)Ca_2Si_8O_{20}$) given the case that all Th is substituted by U. Natural ekanite may form hydrothermally and was found to contain 27% of Th replaced with U [29]. U and Th can substitute freely for one another in the ekanite structure, principally the formation of U-ekanite should be possible [9]; however, a member containing only U was so far not found in nature (which is probably due to the frequent appearance of Th and U together and a resulting preferential Th compound formation). XRD analysis did not prove the presence of the compound so it might be present as amorphous phase.

The observations let conclude that the stability fields in which the formation of the measured phases takes place, can be grouped semi-quantitatively into a scheme which is determined by the concentrations of dissolved silica and the abundance of calcium in solution (shown in Fig. 7). No phase formation was observed at [Si] $<10^{-2}$ mol/l. However at [Si] = 10^{-2} mol/l, the U–Ca–Si phase appears at conditions of virtually unlimited Ca^{2+} supply, whereas the U–Si–Ti–Fe–Ca phase was found at moderate to low $[Ca]_{diss}$ (3×10^{-4} mol/l], and the U–Si phase which is probably coffinite was found in both environments.

On the samples exposed to groundwater with enhanced carbonate content, no secondary phase formation could be observed, and no separate crystalline objects were found. The possible formation of an U(IV) carbonate cannot be ruled out completely, for the SEM–EDX analysis of the surface was not able to detect the presence of C (no ultrathin detector window was used with the instrument). Still, this seems unlikely. The pure U(IV)carbonate $U(CO_3)_2$ is not known. The basic carbonate $UO(CO_3)$ that can be generated in U(IV) solution upon addition of $(NH_4)_2(CO_3)$ (which was reported to be stable [55]), might theoretically have formed but little facts are known about the conditions under which this happens; the substance is not known to form naturally. Therefore, U(IV) carbonate phases were not taken into account in quantitative consideration during the evaluation of the present work. Ca^{2+} incorporation into the UO_2 lattice have to be considered when leaching in high $[Ca^{2+}]_{diss}$ media since Ca contents of 1–2 wt% were observed with several natural UO_2 samples [43]. More often, co-precipitation mechanisms take place when the geochemical conditions are prevailing to form calcite in sufficient amounts as a host phase. During the surface examinations of the samples used in this work, no evidence of an enhanced Ca content on the surface was found. If a substitution reaction took place, it might have been hindered by kinetic factors but it is much more obvious that the stability field of calcite co-precipitation was not reached, since conditions of higher alkalinity are required [11].

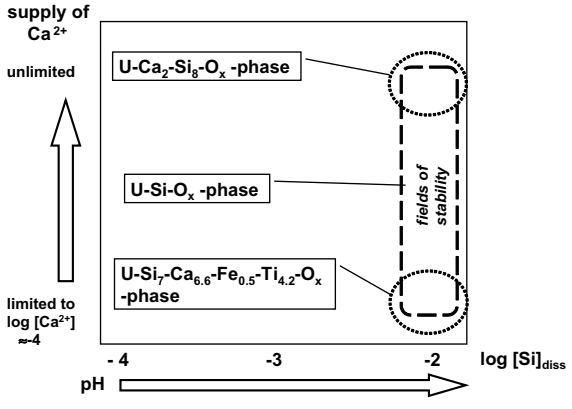

Fig. 7. Semi-quantitative stability scheme of the UO_2 alteration phases observed in this work.

4.5. The role of trace elements: Implications for spent fuel

The actual spent nuclear fuel foreseen for direct disposal into deep underground formations contains a considerable number of elements besides U (which forms the main matrix of this material) in an isotopic composition and mass abundance depending on the irradiation history. Most of these elements are present in a concentration less than 1 wt% but the activity of these radionuclides contributes essentially to the radiotoxicity of the material. The questions about retardation of these elements within the matrix of the material, their incorporation into uranium secondary phases, and the minerals which might be formed by themselves, are of great importance for a safety assessment.

Fission product elements can form a variety of minerals in anoxic environments [54]. The formation of solid phases containing U(IV) and a fission product ion (or severals of these) can therefore be expected when assuming a contact with reactive U surfaces during dissolution processes. Several natural U(IV) minerals are known to contain quantities of a fission product element (some are compiled in Table 6). The knowledge of their solubility products, and their mobilisation behaviour under geochemically relevant conditions, can be regarded as scarce [56]. In addition to the often observed U/Th-REE substitutions, the special cases of Zr, Ru, and Ce4+/An4+ are considered in the following.

Coffinite and zircon ($ZrSiO_4$) are of equivalent crystal structure (a Me^{4+} ion coordinated by eight O atoms in the form of a distorted cube-like polyhedron). They can form solid solutions [46], out of which the release of Zr might be enhanced in comparison to pure zircon. A transformation of UO_2 into $USiO_4$ under geologic conditions will probably result in a different solubility

behaviour for Zr [57,58]. In the case of Ru, Janeczek [59,60] observed no migration during the process of coffinite formation. Fissiogenic Ru, which was found in a coffinite sample from the Bangombe reactor zone of the Oklo prehistoric reactor system, seems to have remained at its original location; however, it is not clear if the coffinite material hosted Ru in its crystal structure. Synthetic brannerite containing Pu or Ce was prepared recently [61,62]. It was found that this material has a different thermodynamic stability field compared to the U brannerites known so far. This will probably influence the dissolution behaviour and should lead to either a preferential or a hindered dissolution of Pu out of the matrix. However, since the synthesis was performed by a melting reaction (in the first case), it is not clear if Pu-Brannerite would form hydrothermally in the presence of dissolved uranium.

Fissiogenic rare earth elements (REE) present in material from the Oklo natural reactors were found to be retained in the UO_2 matrix if the geochemical conditions remain reducing or anoxic. However, since oxidizing conditions enhance dissolution of the UO_2 material, a segregation of REE elements (especially for La and Ce) during their migration pattern was observed [63]. A similar fractionation process, induced by the UO_2 lattice conversion resulting from a reaction with Si, could take place. Since the structural qualities of spent UO_2 fuel are different from these natural materials, it needs still to be demonstrated if similar processes would occur in the case of the fuel material. However we conclude that rare earth and noble metal elements will at least partially be retained in such a matrix also after its alteration as described here. Furthermore, considering our results, hydrothermal formation of brannerite seems not to be the preferential alteration pathway at conditions of high silica activity in the contacting fluids.

The reaction temperature under which these processes take place is of significance for the reaction progress. Elevated temperatures, as simulated in our experiments, can stem either from the decay of the active material in the first thousands of years or, when long times have passed and geologic conditions are changing gradually, from the intrusion of heated fluids. The second case is observed with several uranium deposits (a typical example being the Menzenschwand mine in Germany [64]).

Furthermore, it must be kept in mind that the presence of highly radioactive elements in sufficient amount can induce local redox heterogeneities in the material by the radiolysis of surrounding water [65,66]. This was found at some selected points of the natural fission reactors of Oklo, as well as in laboratory experiments. In the above mentioned Menzenschwand example, Ra from decay processes, accumulated in barium-bearing minerals, induced water radiolysis over some millions of years. The production of a reducing species (for example H_2), as expected during radiolysis processes, has great impact upon the mobilisation behaviour of U from directly disposed spent nuclear fuel [67]. If this is true also for the herein contained Pu or Np remains to be proved, since the dissolution mechanisms of their dioxides are different from those of UO_2.

The question is still open if anoxic alterations, as described here, can take place at all in the presence of highly alpha-active elements such as Pu or Np, and also it is not known if hydrothermal conditions will possibly change the effect of water radiolysis products upon the dissolution process [68]. Ongoing work will be concerned with this problem.

5. Conclusions

The data obtained in this work may provide a base for investigating the complex interactions of fission products, transuranic elements, the UO_2 matrix and groundwater ions in anoxic environments. It is so far not clear if these elements will be incorporated into UO_2 alteration phases in oxygen-free environments or if they will segregate into independent phases. However, the conditions in this study were chosen to provide a scenario of extreme conditions (e.g., temperature, ion concentration), and do not necessarily have to prevail in a possible future repository.

Our findings show that the activity of silica, combined with the temperature at the solid–liquid interface, can control the extent of formation of uranium(IV)silicates, and, hence, the structural qualities of material which is comprised by an UO_2 matrix. Particularly, at elevated temperatures, the influence was observable at laboratory timescales (in experiments conducted with a duration of 1000 h, and longer), and can be summarised by the following:

1. Mechanisms that lead to the alteration and secondary phase formation on UO_2 under anoxic geologic storage conditions differ from those taking place in oxic environments. Generally speaking, lattice incorporation and ion exchange at the UO_2 surface dominate whereas oxidative dissolution, complexation, or hydrolysis are of secondary importance. Carbonate, which is known to strongly complex and dissolve U in oxic conditions, was not found to have a proved effect at low Eh conditions.
2. Of all three reactions investigated, only the interaction with dissolved Si proved to have a measurable effect. The reaction of the UO_2 surface with Si is strongly influenced by the reaction temperature. At elevated temperatures, solid products with a U–Si ratio of 1:1 were measured (matching the elemental composition of the mineral coffinite). XRD analysis gave some evidence for $USiO_4 \cdot nH_2O$ formation but the phase is not properly crystallised and formed

in amounts insufficient to deliver clear signals. A phase containing U, Ca, Si, Fe, and Ti was found in small quantities (matching roughly the composition of a chevkinite-group member). After treatment at ambient temperature, no phase formation could be observed.

3. An additional experiment, during which UO_2 was treated in Si-spiked groundwater in the presence of CaO, TiO_2, Fe_2O_3/Fe(0), resulted in the formation of secondary phases with a constant U–Ca–Si ratio of 1:2:8 (minor quantities of the phase containing U:Si of 1:1 were formed also). Assumed that this is a defined mineral phase, its composition does not coincide with any uranyl mineral. The element ratio is typical for the mineral ekanite $(Th,U)Ca_2Si_8O_{20}$. Free substitution of U for Th in ekanite phases is principally possible.
4. The observed secondary phases were found to form at different geochemical conditions. An analysis of these formation conditions in a semi-quantitative scheme of stability fields shows that (apart from reaction temperature) the parameters $[Si]_{diss}$ and $[Ca]_{diss}$ (delivered from a solid phase) control the reaction pathway.
5. The measured ratio of U oxidation states in some of the experimental solutions (about 25% of U in the +4 state) is in contrast to the nature of the observed phases. The method used cannot be considered completely unquestionable so the ratio of U(VI) may at least in the alkaline experiments, have been well higher. This suggests that the mechanisms leading to a secondary phase formation under anoxic conditions are obviously strongly controlled by near-surface conditions that are, at least partially, independent of the geochemical conditions in the bulk solution.

Acknowledgement

The authors acknowledge Dr U. Kramar of the University Karlsruhe (Institute of Geochemistry and Petrography) for the discussion of the groundwater analyses, Mr J. Jernström for experimental support, and Dr I. Ray for support on SEM interpretation. Drs B. Finch and A. Chakmouradian for detailed considerations on the problem, and Dr C. Ronchi for valuable discussions on the manuscript. An anonymous reviewer helped considerably to improve the manuscript.

References

[1] J.I. Kim, Nucl. Eng. Des. 202 (2000) 143.
[2] W. Miller, R. Alexander, N. Chapman, I. McKinley, J. Smellie, Geological Disposal of Radioactive Wastes & Natural Analogues, Waste Management Series, vol. 2, Pergamon/Elsevier, 2000.
[3] D. Wronkiewicz, J. Bates, S. Wolf, E. Buck, J. Nucl. Mater. 238 (1996) 78.
[4] R. Finch, R. Ewing, J. Nucl. Mater. 190 (1992) 133.
[5] D. Langmuir, Geochim. Cosmochim. Acta 42 (1978) 547.
[6] K. Lieser, Radiochim. Acta 70/71 (1995) 355.
[7] J. Jerden Jr, A. Sinha, Appl. Geochem. 18 (2003) 823.
[8] J. Janeczek, R. Ewing, J. Nucl. Mater. 190 (1992) 157.
[9] R. Finch, T. Murakami, in: P. Burns, R. Finch (Eds.), Uranium: Mineralogy, Geochemistry and the Environment, Reviews in Mineralogy, vol. 38, Mineralogical Society of America, Washington, DC, 1999, p. 91.
[10] M. Goldhaber, B. Hemingway, R. Mohagheghi, R. Reynolds, H. Northrop, Bull. Mineral. 110 (1987) 131.
[11] E. Curti, Appl. Geochem. 14 (1999) 433.
[12] D.W. Shoesmith, J. Nucl. Mater. 282 (2000) 1.
[13] J. Janeczek, R. Ewing, R.C., Mat. Res. Soc. Symp. Proc. 257 (1992) 497.
[14] D. Gallup, F. Sugiaman, V. Capuno, A. Manceau, Appl. Geochem. 18 (2003) 1597.
[15] V. Oversby, SKB Technical Report TR-99-22, SKB, Stockholm, 1999, p. 18.
[16] R. Corey, in: M. Anderson, A. Rubin (Eds.), Adsorption of Inorganics at Solid–liquid Interfaces, Ann Arbor Science, New York, 1981, p. 160.
[17] A. Loida, B. Grambow, H. Geckeis, J. Nucl. Mater. 238 (1996) 11.
[18] M. Fattahi, R. Guillaumont, Radiochim. Acta 61 (1993) 155.
[19] R. Guillaumont, T. Fanghánel, V. Neck, J. Fuger, D. Palmer, I. Grenthe, M. Rand (Eds.), Update on the Chemical Thermodynamics of U, Pu, Np, Am and Tc, NEA-OECD, Chemical Thermodynamics, vol. 5, Elsevier, Amsterdam, 2003, p. 157.
[20] F.B. Milton, J.B. Pearson, CASINO User's Guide and Reference Manual, TRI-DN-89-19, Vancouver, 1989.
[21] J. Quinones, J. Garcia-Serrano, J. Serrano, P. Diaz-Arocas, J. Almazan, Mat. Res. Soc. Symp. Proc. 506 (1998) 247.
[22] J. Choi, S. Hulseapple, M. Conklin, J. Harvey, J. Hydrol. 209 (1998) 297.
[23] C. Jimenez-Lopez, E. Caballero, F. Hromanek, Geochim. Cosmochim. Acta 65 (2001) 3219.
[24] K. Ollila, M. Olin, M. Lipponen, Radiochim. Acta 74 (1996) 9.
[25] H. Dunsmore, S. Hietanen, L. Sillen, Acta Chem. Scand. 17 (1963) 2644.
[26] A. Abdelouas, W. Lutze, H. Nuttall, J. Cont. Hydrol. 36 (2000) 353.
[27] Hj. Matzke, J. Nucl. Mater. 238 (1996) 58.
[28] B. Anderson, G. Claringbull, R. Davis, D. Hill, Nature 190 (4780) (1961) 997.
[29] V. Diella, G. Mannucci, Rend. Soc. Ital. Min. Petr. 41 (1986) 3.
[30] J. Szymanski, J. Scott, Can. Mineral. 20 (1982) 271.
[31] B. Gatehouse, I. Grey, P. Kelly, Amer. Mineralogist 64 (1979) 1010.
[32] R. Macdonald, H. Belkin, Miner. Mag. 66 (2002) 1075.
[33] JCPDS. Powder Diffraction File, 44, 7354-CD ROM (PDF 1-44), International Centre for Diffraction Data, Pennsylvania, 1994.

[34] N. Sturchio, M. Antonio, L. Soderholm, S. Sutton, J. Brannon, Science 281 (1998) 971.
[35] R. Reeder, M. Nugent, C. Tait, D. Morris, S. Heald, K. Beck, et al., Environ. Sci. Technol. 34 (2000) 638.
[36] M. Min, in: M. Cuney, E. von Pechmann, J. Rimsaite, F. Simova, H. Sorensen, S. Augustithis (Eds.), Primary radioactive minerals, Theophrastus Publishing & Proprietary Co., Athens, 1991, p. 75.
[37] I. Grenthe, H. Wanner, I. Forest (Eds.), Chemical Thermodynamics of Uranium, NEA-OECD, Chemical Thermodynamics, vol. 1, North Holland, Amsterdam, 1992, p. 323.
[38] J. Bruno, I. Grenthe, P. Robouch, Inorg. Chim. Acta 158 (1989) 221.
[39] L. Fuchs, H. Hoekstra, The American Mineralogist 44 (1959) 1057.
[40] G. Parks, D. Pohl, Geochim. Cosmochim. Acta 52 (1988) 863.
[41] P. Tremaine, J. Chen, G. Wallace, W. Boivin, J. Sol. Chem. 10 (3) (1981) 221.
[42] M. Amme, B. Renker, B. Schmid, M. Feth, H. Bertagnolli, W. Dóbelin, J. Nucl. Mater. 306 (2002) 202.
[43] F. Shishkova-Simova, in: M. Cuney, E. von Pechmann, J. Rimsaite, F. Simova, H. Sorensen, S. Augustithis (Eds.), Primary radioactive minerals, Theophrastus Publishing & Proprietary Co., Athens, 1991, p. 217.
[44] B. De Vivo, F. Ippolito (Eds.), Uranium Geochemistry, Mineralogy, Geology, Exploration and Resources, The Institution of Mining and Metallurgy, London, 1984, p. 15.
[45] H. Hoekstra, L. Fuchs, Science 1 (1956) 123.
[46] C. Keller, Úber die Festkórperchemie der Actiniden-Oxide, KfK-Report 225, Kernforschungszentrum Karlsruhe, 1964.
[47] F. Shishkova-Simova, R. Petrova, in: M. Cuney, E. von Pechmann, J. Rimsaite, F. Simova, H. Sorensen, S. Augustithis (Eds.), Primary radioactive minerals, Theophrastus Publishing & Proprietary Co., Athens, 1991, p. 235.
[48] F. Mazzi, R. Munno, Amer. Mineralogist 68 (1983) 262.
[49] J. Rimsaite, in: M. Cuney, E. von Pechmann, J. Rimsaite, F. Simova, H. Sorensen, S. Augustithis (Eds.), Primary radioactive minerals, Theophrastus Publishing & Proprietary Co., Athens, 1991, p. 105.
[50] A. Speer, Rev. Mineral. 5 (1982) 113.
[51] M. Inagaki, T. Morishita, M. Hirano, V. Gupta, T. Nakajima, Solid State Ionics 156 (2003) 275.
[52] G. Lumpkin, J. Nucl. Mater. 289 (2001) 136.
[53] J. Janeczek, N. Jb. Miner. Mh. H 9 (1991) 385.
[54] R. Gaines, H. Skinner, E. Foord, A. Rosenzweig, Dana's New Mineralogy, Eigth ed., John Wiley & Sons, New York, 1997.
[55] B. Sahoo, D. Patnaik, Nature 4714 (1960) 683.
[56] I. Grenthe, Radiochim. Acta 52/53 (1991) 425.
[57] T. Geisler, R. Pidgeon, W. Van Bronswijk, R. Kurtz, Chem. Geol. 191 (2002) 141.
[58] B. Jensen, J. Cont. Hydr. 13 (1993) 231.
[59] J. Janeczek, R.C. Ewing, V.M. Oversby, L.O. Werme, J. Nucl. Mater. 238 (1996) 121.
[60] J. Janeczek, in: P. Burns, R. Finch (Eds.), Uranium: Mineralogy, Geochemistry and the Environment, Reviews in Mineralogy, vol. 38, Mineralogical Society of America, Washington, DC, 1999, p. 321.
[61] V. Yudintsev, T. Yudintseva, in: Proceedings of the ICEM 01 8th international conference on radioactive waste management and environmental remediation, Bruges, Belgium, 2001.
[62] K. Helean, A. Navrotsky, G. Lumpkin, M. Colella J. Lian, R. Ewing, et al., J. Nucl. Mater. 320 (2003) 231.
[63] H. Hidaka, F. Gauthier-Lafaye, Geochim. Cosmochim. Acta 64 (2000) 2093.
[64] B. Hofmann, Nagra, Technical Report No. 88-30, Baden, 1989, p. 174.
[65] V. Savary, M. Pagel, Geochim. Cosmochim. Acta 61 (21) (1997) 4479.
[66] V. Rondinella, Hj. Matzke, J. Cobos, T. Wiss, Mat. Res. Soc. Symp. Proc. 556 (1999) 447.
[67] E. Shock, D. Sassani, H. Betz, Geochim. Cosmochim. Acta 61 (20) (1997) 4245.
[68] K. Ishigure, Y. Katsumura, G. Sunaryo, D. Hiroishi, Radiat. Phys. Chem. 46 (1995) 557.
[69] G. Perrault, J. Szymanski, Can Mineral. 20 (1982) 59.
[70] S. Hanson, Mineral. Mag. 63 (1999) 27.